Research Article

Magnetoelectric effect in three-layered gradient LiNbO$_3$/Ni/Metglas composites

Viktor V. Kuts[1], Andrei V. Turutin[1], Aleksandr M. Kislyuk[1], Ilya V. Kubasov[1],
Roman N. Zhukov[1], Alexander A. Temirov[1], Mikhail D. Malinkovich[1], Nikolai A. Sobolev[1,2],
Yuri N. Parkhomenko[1,3]

1 *Laboratory of Physics of Oxide Ferroelectrics, National University of Science and Technology MISiS, 4-1 Leninsky Ave., Moscow 119049, Russian Federation*

2 *Department of Physics and I3N, University of Aveiro, 3810-193 Aveiro, Portugal*

3 *Federal State Research and Development Institute of Rare Metal Industry (Giredmet JSC), 2-1 Elektrodnaya Str., Moscow 111524, Russian Federation*

Corresponding author: Viktor V. Kuts (viktor.kuts.3228@yandex.ru) and Andrei V. Turutin (aturutin92@gmail.com)

Citation: Kuts VV, Turutin AV, Kislyuk AM, Kubasov IV, Zhukov RN, Temirov AA, Malinkovich MD, Sobolev NA, Parkhomenko YuN (2022) Magnetoelectric effect in three-layered gradient LiNbO$_3$/Ni/Metglas composites. *Modern Electronic Materials* 8(4): 141–147. https://doi.org/10.3897/j.moem.8.4.98951

Abstract

The effect of annealing in a permanent magnetic field on the magnitude of magnetoelectric coefficient in three-layered gradient magnetoelectric LiNbO$_3$/Ni/Metglas composites has been studied. A method of electrochemical nickel deposition on bidomain lithium niobate crystals has been demonstrated. We show that the optimum annealing temperature in a permanent magnetic field for the generation of the highest remanence in the Ni layer is 350 °C. The specimens annealed at this temperature exhibit the greatest shift of the magnetoelectric coefficient dependence on external magnetic field magnitude relative to the value $H_{dc} = 0$. The quasi-static magnetoelectric coefficient in the absence of an external magnetic field proves to be 1.2 V/(cm · Oe). The highest magnetoelectric coefficient that has been achieved at a bending structure resonance frequency of 278 Hz proves to be 199.3 V/(cm · Oe) without application of an external magnetic field. The experimental magnetoelectric coefficient figures for three-layered gradient LiNbO$_3$/Ni/Metglas composites are not inferior to those for most magnetoelectric composite materials reported earlier.

Keywords

magnetoelectric effect, composite structures, magnetizing layer, bidomain lithium niobate, Metglas, nickel

1. Introduction

The magnetoelectric (**ME**) effect consists in a change in material polarization under the influence of an external magnetic field (direct effect) or a change in material magnetization in the presence of an electric field (inverse effect) [1]. Interest to composite ME materials is caused by the possibility of fabricating based on them a wide range of devices exhibiting unique properties such as microwave phase shifting devices, electrically tunable RF resonators and delay lines, energy harvesting systems, ME non-volatile memory, micromechanical ME antennas, ME gyrators and ultra-sensitive magnetic field sensors [2–6].

The highest ME coefficient is observed in composite structures consisting of piezoelectric and magnetostrictive

layers [7]. Magnetoelectric composites in which piezo-electric materials are coated (using different methods, i.e., magnetron sputtering, electrochemical deposition or epoxy resin bonding) with amorphous metals (Metglas) exhibit the highest ME coefficients [7]. To achieve the highest ME coefficient structures should be exposed to an external constant **(DC)** magnetizing field (working point). This is since the piezomagnetic coefficient (q) is a nonlinear function of a DC magnetic field with the peak value being achieved at a specific optimumagnetic field magnitude. Typically an external magnetizing field is applied using solenoids, Helmholtz coils or permanent magnets located at a distance from the ME specimen. The necessity of applying an external magnetic field for efficient work of ME composites is a noticeable disadvantage of these materials leading to an increase in the dimensions of the devices.

Several methods of achieving the working point of ME composites without the use of external DC magnetic field sources have been described in literature. One method is to produce mechanical stresses in the ME structure [8, 9]. Preliminary mechanical deformation of the ME structure causes a change in the magnetostrictive coefficient, which leads, under a certain configuration, to the maximum value of q [9]. Another method of shifting the magnetostrictive coefficient to the working point is the use of additional magnetic layers that affect the magnetostrictive phase due to their own remanence magnetization. Local laser heating of the magnetostrictive layer (Metglas) was used for forming a surface layer with a recrystallized material containing the α-Fe phase [10]. This phase after placing it in a DC magnetic field retains remanence magnetization, which can affect the more magnetically soft metglas, and therefore generate a non-zero ME coefficient in the absence of an external magnetic field. It was demonstrated [11] that a non-zero ME effect can be generated in a three-layered Metglas/Ni/PZT structure without applying an external magnetic field due to the impact of remanence magnetization of the more magnetically hard material (nickel) on the more magnetically soft material (Metglas). A ME coefficient of 1.6 V/(cm·Oe) was achieved. Thin antiferromagnetic $Mn_{70}Ir_{30}$ layers can also be used as magnetizing layers [12].

We showed earlier that the use of bidomain lithium niobate (LiNbO₃, **LN**) crystals as a piezoelectric phase in composite ME materials provides for a significant increase in the ME coefficient [13, 14].The best samples have a record sensitivity to an alternating magnetic field among other composite ME materials, the limit of magnetic field detection in the work [15] was 92 fT/Hz$^{1/2}$ at a bending resonance frequency of 6862 Hz. Since the noise of external acoustic vibrations dramatically reduces the magnetic field sensitivity of ME structures, we developed and tested ME sensor in the form of a tuning-fork [16]. When using a sensitive element based on the ME composite in the form of a tuning fork, the acoustic signal and thermal excitations are effectively suppressed. This design reduces the influence of external vibrational noise

up to 7 times and increases the sensitivity to the magnetic field compared to a single ME sensor.

In this work, we present the results of testing the technology of nickel electrochemical deposition on LN $Y + 128°$-cut plates and studying the effect of annealing in a DC magnetic field on the ME coefficient in three-layer gradient composites LiNbO₃/Ni/Metglas.

2. Experimental

The basis of the ME structures were $Y + 128°$-cut LN crystals. Nickel layer annealing modes were tested for specimens having $5 \times 30 \times 0.5$ mm³ linear dimensions. After the optimum annealing mode was found the measurements were carried out for a longer specimen having $5 \times 50 \times 0.5$ mm³ dimensions. The use of a longer structure allows one to reduce the resonance bending mode frequency and increase the low-frequency magnetic field sensitivity of the ME structure which is important for further biomedical device applications [17]. Ferroelectric bidomain structures were formed in the LN plates using diffusion annealing [13]. Nickel which was used as a magnetizing layer was applied onto the LN bidomain crystals by electrochemical deposition. The electrode for deposition process was a 100 nm thick titanium film deposited onto one side of the crystal by magnetron sputtering. After the nickel layer was deposited on LN surface the samples were annealed in a DC magnetic field. The magnetostrictive layer Metglas 2826 MB was bonded on the LN/nickel structures using epoxy glue after annealing in a DC magnetic field.

2.1. Electrochemical deposition

Schematic of the electrochemical deposition plant is shown in Fig. 1. The power source *1* generates stable current between the nickel anode *3* and the bidomain LN crystal *4* that are placed in the solution *2*.

Electrochemical deposition was performed at 65 °C. The solution consists of nickel sulfate (300 g/l concentration) and boric acid (90 g/l). The current in the circuit was limited to 25 mA.
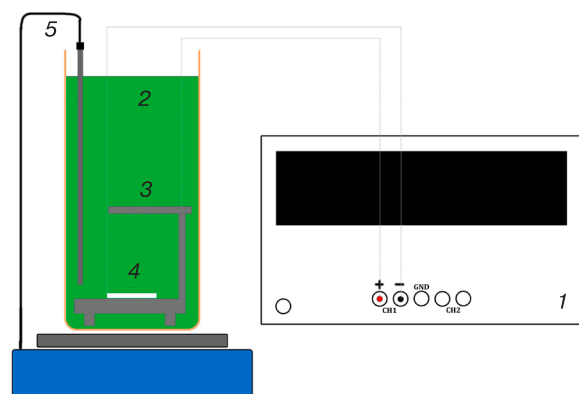

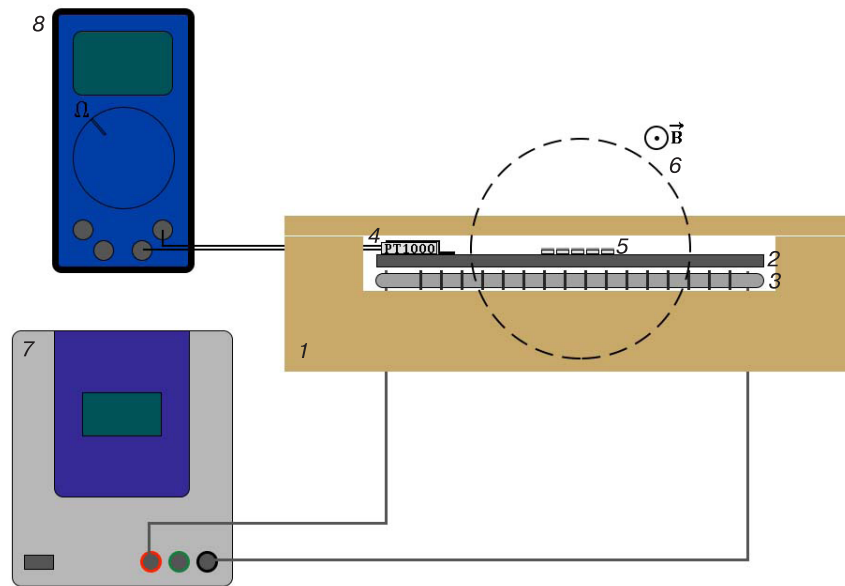**Figure 1.** Schematic of nickel electrochemical deposition plant

Figure 2. Schematic of installation for annealing of ME structures in permanent magnetic field: (*1*) external furnace enclosure; (*2*) aluminum heat distributor; (*3*) heating element; (*4*) PT1000 thermistor; (*5*) specimens; (*6*) external uniform magnetic field; (*7*) power source; (*8*) multimeter

The electrochemical deposition rate depends on a number of parameters including the area of the target surface, and therefore it differs for different specimens. For example, the deposition rate for the 50 mm long specimens was 1 mm/min, whereas for the 30 mm long specimens it was 1.3 mm/min. The final nickel layer thickness was 10 mm for each sample.

2.2. Annealing in permanent magnetic field

Schematic of the installation for annealing in a permanent magnetic field is shown in Fig. 2. The outer enclosure *1* is made from firebrick. Electric current generated by the power source *7* passes through the nichrome wire of the heating element *3* and heats up the aluminum distributor *2*. The specimens *5* are placed along the force lines of the applied external magnetic field *6*.

For understanding the impact of annealing temperature on the ME properties of the specimens we carried out a series of anneals at 350, 360, 380 and 390 °C for 2 min. The external magnetic field induction was 330 mT.

2.3. ME effect measurement method

Schematic diagram of the measuring setup of ME effect is shown in Fig. 3. The lock-in detector *1* feeds an alternating sine signal to the Helmholtz coils *2*. The test specimen *3* is deformed by the alternating magnetic field and as a result a potential difference occurrs in the electrodes of the LN piezoelectric crystal which is detected by the lock-in. The measurement process is computer-assisted, the data being stored in the computer memory *4*.

In the series of quasi-static measurements the magnitude of the applied DC external magnetic field varied in the range from –8 to 8 Oe, the amplitude and frequency

of the alternating magnetic field being 0.1 Oe and 117 Hz, respectively. Dynamic measurements were carried out in the 10 Hz – 1 kHz frequency range by applying analternating magnetic field with a 0.1 Oe amplitude. Each specimen was tested by applying the optimum DC magnetic field and without a DC magnetic field.

3. Results and discussion

Results of quasi-static ME coefficient α measurements for the $5 \times 30 \times 0.5$ mm³ specimens annealed in a magnetic field at different temperatures are shown in Fig. 4. The ME coefficients without DC magnetic field application for different specimens vary from 0.1 to 0.2 V/(cm · Oe). There is a consecutive shift of the ME coefficient *vs* magnetic field curve toward $H_{dc} = 0$ with an increase in the specimen annealing temperature. For example, the great-
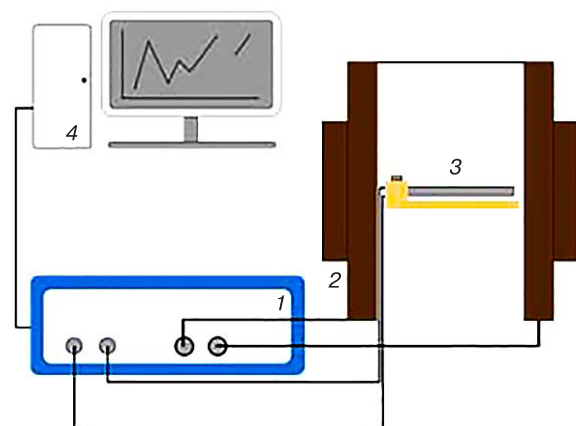

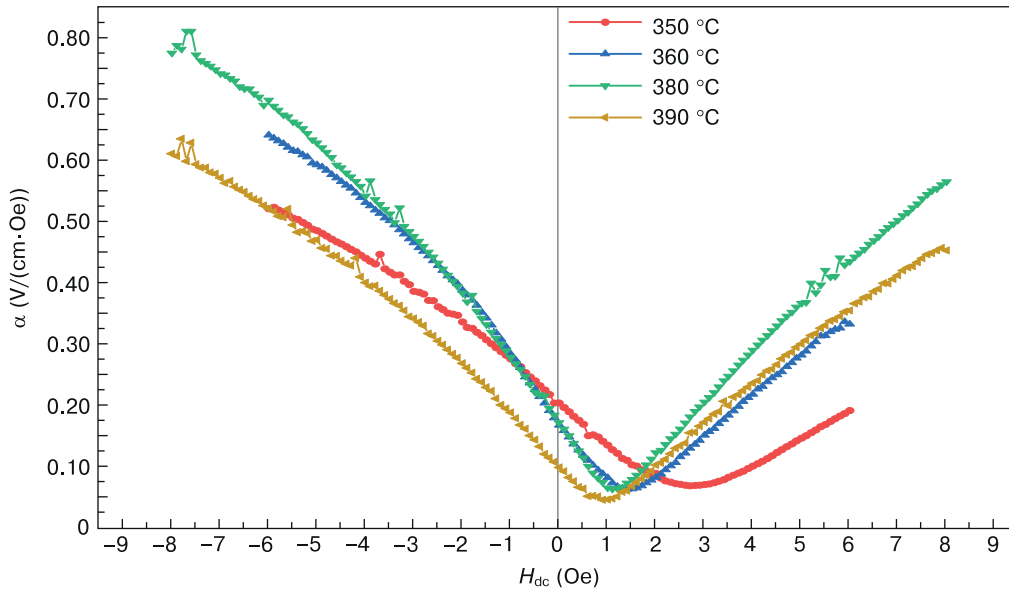**Figure 3.** Schematic diagram of ME coefficient measuring setup

Figure 4. Results of quasi-static ME coefficient measurements forLiNbO$_3$/Ni/Metglas structures annealed at different temperatures in a permanent magnetic field
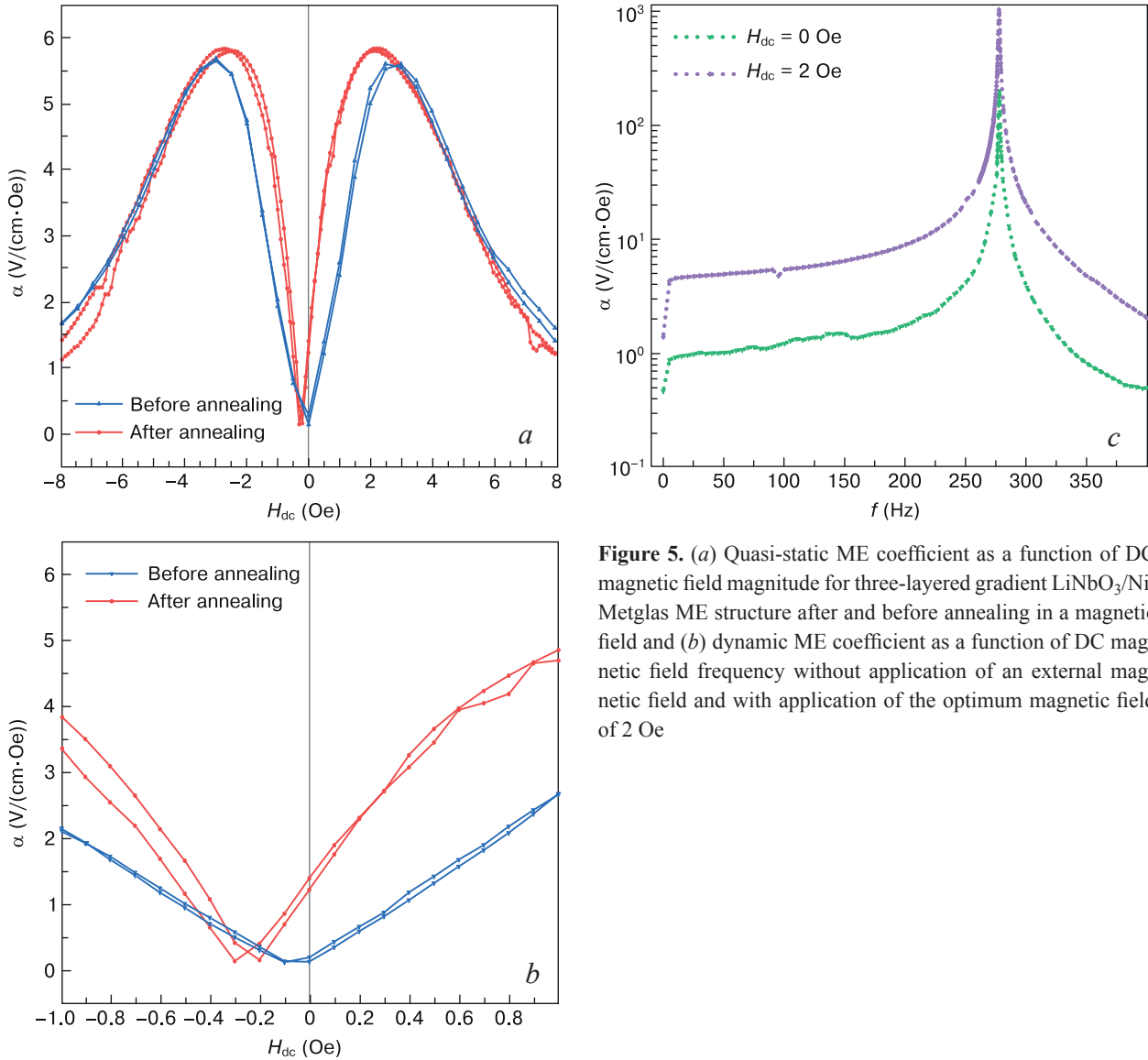

Figure 5. (*a*) Quasi-static ME coefficient as a function of DC magnetic field magnitude for three-layered gradient LiNbO$_3$/Ni/Metglas ME structure after and before annealing in a magnetic field and (*b*) dynamic ME coefficient as a function of DC magnetic field frequency without application of an external magnetic field and with application of the optimum magnetic field of 2 Oe

est shift of the curve relative to the origin of coordinates was 2.8 Oe and observed for the specimen annealed in a magnetic field at 350 °C. The smallest curve shift (1 Oe) was observed for the specimen annealed in a magnetic field at 390 °C. Later on, when fabricating the 50 mm long specimen we used annealing at 350 °C in order to achieve the greatest non-zero ME coefficient without applying an external DC magnetic field.

After finding the optimum annealing parameters we measured the quasi-static and dynamic ME coefficients for the 50 mm long structure under a magnetizing layer before and after annealing. The specimen was annealed in an external magnetic field at 350 °C. The measurement results are illustrated in Fig. 5.

The results of ME coefficient measurements as a function of DC magnetic field magnitude are shown in Fig. 5 a. After annealing the ME coefficient curve shifted through 0.3 Oe to the right-hand side which caused a non-zero ME effect in the absence of an external permanent magnetic field. The ME coefficient at $H_{dc} = 0$ was 1.2 V/(cm · Oe). Furthermore, the greatest ME coefficient at the optimum magnetic field with a magnitude of about 2 Oe increased to about 5.8 V/(cm · Oe) after annealing.

Figure 5 b shows results of ME coefficient measurements as a function of DC magnetic field frequency. The measurements were carried out at the optimum permanent magnetic field of 2 Oe and without application of an external magnetic field. The greatest ME coefficient was achieved at a structure bending resonance frequency of 278 Hz. The ME coefficient without application of an external magnetic field was 199 V/(cm · Oe) and at the optimum magnetic field it was 1024 V/(cm · Oe).

The Table 1 below shows a comparison between the current experimental and earlier literary data on the quasi-static and dynamic (at the resonance frequency) ME coefficient without application of an external magnetic

Table 1. Comparison between ME coefficients for different composite structures without application of an external magnetic field ($H_{dc} = 0$)

ME composite	α (V/(cm · Oe))	
	Quasi-static	Dynamic
FeCuNbSiB/Ni–PZT-FeCuNbSiB/Ni [18]	–	183.2 (at f_r = 158.34 kHz)
FeCuNbSiB/Terfenol-D/Be-bronze/PZT [19]	20 (at f_{AC} = 37 kHz)	0.33 (at f_r = 1300 Hz); 11.5 (at f_r = 37 kHz)
Ni/PZT/FeNi [20]	0.225 (at f_{AC} = 1 kHz)	–
FeNi/PZT/Ni ring-shaped [21]	0.035 (at f_{AC} = 1 kHz)	–
Metglas/PZT/Ni with neodymium magnet in the form of weight at cantilever end [22]	–	55.7 (at f_r = 270 Hz)
Partially annealed Metglas/PMN-PZT [23]	20 (at f_{AC} = 1 kHz)	1220 (at f_r = 23.32 kHz)
$CFO_{0.55}$–$CNT_{0.1}$–$PVDF_{0.35}$/P(VDF-TrFE)/ $CFO_{0.55}$–$CNT_{0.1}$–$PVDF_{0.35}$ [24]	0.0167 (at f_{AC} = 1 kHz)	–
NKNLS-NZF/Ni/NKNLS-NZF [25]	11.78 (at f_{AC} = 100 Hz)	27.3 (at f_r = 23.32 kHz, H_{dc} = 34 Oe)
FeCuNbSiB/Terfenol-D/Be-bronze/PMN-PT [26]	20 (at f_{AC} = 31 kHz)	33 (at f_r = 23.13 kHz)
Ta–Pt–AlN–Cr–Au/Si/Ta–Cu–Mn_3Ir–$(Fe_{90}Co_{10})_{78}Si_{12}B_{10}$–Ta–Cu–$Mn_3Ir$–$(Fe_{90}Co_{10})_{78}Si_{12}B_{10}$ [27]	0.3 (at f_{AC} = 797 Hz)	–
$SrFe_{12}O_{19}$/Metglas/PZT [28]	1 (at f_{AC} = 1 kHz)	29 (at f_r = 120 kHz)
Metglas/PVDF/Ni [29]	–	38.24 (at f_r = 48.8 kHz)
Metglas/Terfenol-D/PZT [30]	–	16 (at f_r = 40 kHz)
PZT/Ni/Metglas [11]	1.6 (at f_{AC} = 100 Hz)	15 (at f_r = 170 Hz)
Metglas/PZT/Metglas [31]	12 (at f_{AC} = 1 kHz)	380 (at f_r = 33.7 kHz)
PZT/NZFO/PZT [32]	0.037 (at f_{AC} = 1 kHz)	–
AlN/Ta–Cu–$Mn_{70}Ir_{30}$–$Fe_{70.2}Co_{7.8}Si_{12}B_{10}$ [12]	–	96.7 (at f_r = 1197 Hz)
$LiNbO_3$/Ni/Metglas	1.2 (at f_{AC} = 117 Hz)	199.3 (at f_r = 278 Hz)

Notations: f_{AC} is the magnetic field modulation frequency for quasi-static ME effect measurement; f_r is the structure bending resonance frequency.

field for different ME composite structure configurations.

The ME coefficients of three-layered gradient LiNbO$_3$/Ni/Metglas composites obtained in this work are not inferior to those of most ME composites. Only the structures based on lead-containing piezoelectric ceramics (PZT) exhibit greater ME coefficient values. The three-layered gradient LiNbO$_3$/Ni/Metglas composites reported in this work require optimization of the ratio between the Ni and Metglas layer thicknesses for increasing the ME coefficient without application of an external magnetic field.

4. Conclusion

A technology of nickel deposition on bidomain $Y + 128°$-cut LN crystals was presented. The effect of annealing of electrochemically deposited nickel layers in a permanent magnetic field on the ME coefficient of the structures was demonstrated. The optimum annealing temperature was found to be 350 °C. At this temperature the greatest shift of the ME coefficient curves relative to $H_{dc} = 0$ was achieved. After finding the optimum annealing parame-

ters we measured the quasi-static and dynamic ME coefficients for a 50 mm long structure with a magnetizing nickel layer before and after annealing. The ME coefficient at $H_{dc} = 0$ was 1.2 V/(cm · Oe) for a ME coefficient curve shift by field through 0.3 Oe. The greatest ME coefficient was achieved at a bending resonance frequency of 278 Hz. Without application of an external magnetic field the ME coefficient was 199.3 V/(cm · Oe). The results obtained in this work can compete with those for earlier reported structures. Further increase of the ME coefficient without application of an external magnetic field can be achieved by obtaining the optimum ratio between the nickel and Metglas layer thicknesses, avoiding a glue bonding layer between the nickel and Metglas layers and changing the composition of the magnetizing layer (i.e., using higher remanence materials).

Acknowledgment

References

1. Eerenstein W., Mathur N.D., Scott J.F. Multiferroic and magnetoelectric materials. *Nature*. 2006; 442: 759–765. https://doi.org/10.1038/nature05023

2. Vopson M.M. Fundamentals of multiferroic materials and their possible applications. *Critical Reviews in Solid State and Materials Sciences*. 2015; 40: 223–250. https://doi.org/10.1080/10408436.2014.992584

3. Nan C.W., Bichurin M.I., Dong S., Viehland D., Srinivasan G. Multiferroic magnetoelectric composites: historical perspective, status, and future directions. *Journal of Applied Physics*. 2008; 103(3): 031101–031136. https://doi.org/10.1063/1.2836410

4. Bichurin M., Viehland D., Srinivasan G. Magnetoelectric interactions in ferromagnetic-piezoelectric layered structures: Phenomena and devices. *Journal of Electroceramics*. 2007; 19(4): 243–250. https://doi.org/10.1007/s10832-007-9058-x

5. Tu C., Chu Z.-Q., Spetzler B., Hayes P., Dong C.-Z., Liang X.-F., Chen H.-H., He Y.-F., Wei Y.-Y., Lisenkov I., Lin H., Lin Y.-H., McCord J., Faupel F., Quandt E., Sun N.-X. Mechanical-resonance-enhanced thin-film magnetoelectricheterostructures for magnetometers, mechanical antennas, tunable RF inductors, and filters. *Materials (Basel)*. 2019; 12(14): 22–52. https://doi.org/10.3390/ma12142259

6. Fiebig M. Revival of the magnetoelectric effect. *Journal of Physics D: Applied Physics*. 2005: 38(8): 123–152. https://doi.org/10.1088/0022-3727/38/8/R01

7. Palneedi H., Annapureddy V., Priya S., Ryu J. Status and perspectives of multiferroic magnetoelectric composite materials and applications. *Actuators*. 2016; 5(1): 9–40. https://doi.org/10.3390/act5010009

8. Yang S., Xu J., Zhang X., Fan S., Zhang C., Huang Y., Li Q., Wang X., Cao D., Xu J. Self-biased Metglas/PVDF/Ni magnetoelectric laminate for AC magnetic sensors with a wide frequency range. *Journal of Physics D: Applied Physics*. 2022; 55(17): 175002–175003. https://doi.org/10.1088/1361-6463/ac4cf5

9. Jing W.Q., Fang F. Stress-induced self-biasing of magnetoelectric coupling in embedded Ni/PZT/FeNi composite. *Applied Physics Letters*. 2015; 106(21): 212901–212902. https://doi.org/10.1063/1.4921743

10. Pourhosseiniasl M., Yu Z., Chu Z., Yang J., Xu J., Hou Y., Dong S. Enhanced self-bias magnetoelectric effect in locally heat-treated ME laminated composite. *Applied Physics Letters*. 2019; 115(11): 112901–112902. https://doi.org/10.1063/1.5116625

11. Mandal S.K., Sreenivasulu G., Petrov V.M., Srinivasan G. Magnetization-graded multiferroic composite and magnetoelectric effects at zero bias. *Physical Review B: Condensed Matter and Materials Physics*. 2011; 84(1): 011432–014440. https://doi.org/10.1103/PhysRevB.84.014432

12. Lage E., Kirchhof C., Hrkac V., Kienle L., Jahns R., Knöchel R., Quandt E., Meyners D. Biasing of magnetoelectric composites. *Nature Materials*. 2012; 11(6): 523–529. https://doi.org/10.1038/nmat3306

13. Kubasov I.V., Kislyuk A.M., Turutin A.V., Malinkovich M.D., Parkhomenko Y.N. Bidomain ferroelectric crystals: properties and prospects of application. *Russian Microelectronics*. 2021; 50(8): 571–616. https://doi.org/10.1134/S1063739721080035

14. Turutin A.V., Kubasov I.V., Kislyuk A.M., Kuts V.V., Malinkovich M.D., Parkhomenko Y.N., Sobolev N.A. Ultra-sensitive magnetoelectric sensors of magnetic fields for biomedical applica-

tions. *Nanobiotechnology Reports.* 2022; 17: 261–289. https://doi.org/10.1134/S2635167622030223

15. Turutin A.V., Vidal J.V., Kubasov I.V., Kislyuk A.M., Malinkovich M.D., Parkhomenko Y.N., Kobeleva S.P., Pakhomov O.V., Kholkin A.L., Sobolev N.A. Magnetoelectric metglas/bidomain $y + 140°$-cut lithium niobate composite for sensing FT magnetic fields. *Applied Physics Letters.* 2018; 112(26): 262906–263100. https://doi.org/10.1063/1.5038014

16. Turutin A.V., Vidal J.V., Kubasov I.V., Kislyuk A.M., Kiselev D.A., Malinkovich M.D., Parkhomenko Y.N., Kobeleva S.P., Kholkin A.L., Sobolev N.A. Highly sensitive magnetic field sensor based on a metglas/bidomain lithium niobate composite shaped in form of a tuning fork. *Journal of Magnetism and Magnetic Materials.* 2019; 486: 165209–165253. https://doi.org/10.1016/j.jmmm.2019.04.061

17. Liang X., Matyushov A., Hayes P., Schell V., Dong C., Chen H., He Y., Will-Cole A., Quandt E., Martins P., Mccord J., Medarde M., Lanceros-Méndez S., Van Dijken S., Sun N., Sort J. Roadmap on magnetoelectric materials and devices. *IEEE Transactions of Magnetics.* 2021; 57(8): 4000157–400400213. https://doi.org/10.1109/TMAG.2021.3086635

18. Huang D., Lu C., Han B., Wang X., Li C., Xu C., Gui J., Lin C. Giant self-biased magnetoelectric coupling characteristics of three-phase composite with end-bonding structure. *Applied Physics Letters.* 2014; 105(1): 0263502–0263507. https://doi.org/10.1063/1.4904799

19. Zhang H., Lu C., Sun Z. Large self-biased magnetoelectric response in four-phase heterostructure with multiple low-frequency peaks. *Applied Physics Letters.* 2015; 106(3): 033505–0335101. https://doi.org/10.1063/1.4906414

20. Jing W.Q., Fang F. Stress-induced self-biasing of magnetoelectric coupling in embedded Ni/PZT/FeNi composite. *Applied Physics Letters.* 2015; 106(21): 212901–212902. https://doi.org/10.1063/1.4921743

21. Kumar A., Arockiarajan A. Temperature dependent magnetoelectric (ME) response in press-fit FeNi/PZT/Ni self-biased ring composite. *Journal of Applied Physics.* 2019; 106(9): 094102–094103. https://doi.org/10.1063/1.5108708

22. Deka B., Lee Y.W., Yoo I.R., Gwak D.W., Cho J., Song H.C., Choi J.J., Hahn B.D., Ahn C.W., Cho K.H. Designing ferroelectric/ferromagnetic composite with giant self-biased magnetoelectric effect. *Applied Physics Letters.* 2019; 115(19): 192901–192903. https://doi.org/10.1063/1.5128163

23. Pourhosseiniasl M.J., Yu Z., Chu Z., Yang J., Xu J.J., Hou Y., Dong S. Enhanced self-bias magnetoelectric effect in locally heat-treated ME laminated composite. *Applied Physics Letters.* 2019; 115(11): 112901–112902. https://doi.org/10.1063/1.5116625

24. Jing W.Q., Fang F. A flexible multiferroic composite with high self-biased magnetoelectric coupling. *Composites Science and Technology.* 2017; 153: 145–150. https://doi.org/10.1016/j.compscitech.2017.10.010

25. Yang S.C., Park C.S., Cho K.H., Priya S. Self-biased magnetoelectric response in three-phase laminates. *Journal of Applied Physics.* 2010; 108(9): 093706-6. https://doi.org/10.1063/1.3493154

26. Huang D., Lu C., Bing H. Multipeak self-biased magnetoelectric coupling characteristics in four-phase Metglas/Terfenol-D/Be-bronze/PMN-PT structure. *AIP Advances.* 2015; 5(4): 047140–047147. https://doi.org/10.1063/1.4919248

27. Jovičević K.M., Thormählen L., Röbisch V., Toxværd S.D., Höft M., Knöchel R., Quandt E., Meyners D., McCord J. Antiparallel exchange biased multilayers for low magnetic noise magnetic field sensors. *Applied Physics Letters.* 2019; 114(19): 192410–192429. https://doi.org/10.1063/1.5092942

28. Ma J.N., Xin C.Z., Ma J., Lin Y.H., Nan C.W. A cost-effective self-biased magnetoelectric effect in $SrFe_{12}O_{19}$/Metglas/$Pb(Zr,Ti)O_3$ laminates. *Journal of Physics D: Applied Physics.* 2016; 49(40): 405002–405007. http://dx.doi.org/10.1088/0022-3727/49/40/405002

29. Yang S., Xu J., Zhang X., Fan S., Zhang Ch.-Y., Huang Y.-C., Li Q., Wang X., Cao D., Li Sh. Self-biased Metglas/PVDF/Ni magnetoelectric laminate for AC magnetic sensors with a wide frequency range. *Journal of Physics D: Applied Physics.* 2022;55(17): 175002–175003. https://doi.org/10.1088/1361-6463/ac4cf5

30. Chen L., Li P., Wen Y., Zhu Y. Near-flat self-biased magnetoelectric response in three-phase Metglas/Terfenol-D/PZT-laminated composites. *IEEE Transactions on Magnetics.* 2015; 51(11). https://doi.org/10.1109/TMAG.2015.2451140

31. Li M., Wang Z., Wang Y., Li J., Viehland D. Giant magnetoelectric effect in self-biased laminates under zero magnetic field. *Applied Physics Letters.* 2013; 102(8): 082404–082601. https://doi.org/10.1063/1.4794056

32. Mandal S.K., Sreenivasulu G., Petrov V.M., Srinivasan G. Flexural deformation in a compositionally stepped ferrite and magnetoelectric effects in a composite with piezoelectrics. *Applied Physics Letters.* 2010; 96(19): 192502. https://doi.org/10.1063/1.3428774